Eur. Phys. J. B **48**, 409–416 (2005)
DOI: 10.1140/epjb/e2005-00410-2

THE EUROPEAN PHYSICAL JOURNAL B

# Quantum size effects in $\delta$-Pu (110) films

H. Gong and A.K. Ray[a]

Physics Department, University of Texas at Arlington, Arlington, Texas 76019, USA

Received 1st July 2005
Published online 23 December 2005 – 

**Abstract.** First-principles full-potential linearized-augmented-plane-wave (FP-LAPW) calculations have been carried out for $\delta$-Pu (110) films up to seven layers. The layers have been studied at the non-spin-polarized-no-spin-orbit coupling (NSP-NSO), non-spin-polarized-spin-orbit coupling (NSP-SO), spin-polarized-no-spin-orbit coupling (SP-NSO), spin-polarized-spin-orbit coupling (SP-SO), antiferromagnetic-no-spin-orbit coupling (AFM-NSO), and antiferromagnetic-spin-orbit-coupling (AFM-SO) levels of theory. The ground state of $\delta$-Pu (110) films is found to be at the AFM-SO level of theory and the surface energy is found to rapidly converge. The semi-infinite surface energy for $\delta$-Pu (110) films is predicted to be 1.41 J/m$^2$, while the magnetic moments show an oscillating behavior, gradually approaching the bulk value of zero with increase in the number of layers. Work functions indicate a strong quantum size effect up to and including seven layers. The work function of the seven-layer $\delta$-Pu (110) film at the ground state is found to be 2.99 eV.

**PACS.** 71.15.-m Methods of electronic structure calculations – 71.27+a Strongly correlated electron systems; heavy fermions – 73.20.At Surface states, band structure, electron density of states – 75.50.Ee Antiferromagnetics

## 1 Introduction

During the past two decades, considerable theoretical efforts have been devoted to studying the electronic structures and related properties of surfaces to high accuracy. One of the many motivations for this burgeoning effort has been a desire to understand the detailed mechanism that lead to surface corrosion in the presence of environmental gases; an issue that is not only scientifically and technologically challenging but also environmentally important. Such efforts are particularly important for systems like the actinides for which experimental work is relatively difficult to perform due to material problems and toxicity.

Among the actinides, Plutonium (Pu) has attracted extraordinary scientific and technological interests because of its unique properties [1–10]. First, Pu has, at least, six stable allotropes between room temperature and melting at atmospheric pressure, indicating that the valence electrons can hybridize into a number of complex bonding arrangements. Second, plutonium undergoes a 25 percent increase in volume when transformed from its $\alpha$-phase (which is stable below 400 K) to $\delta$-phase (stable at around 600 K), an effect which is crucial for issues of long-term storage and disposal. Third, plutonium represents the boundary between the light actinides, Th to Pu, characterized by itinerant $5f$ electron behavior, and the heavy actinides, Am and beyond, characterized by localized $5f$ electron behavior. In fact, the high temperature fcc $\delta$-phase of plutonium exhibits properties that are intermediate between the properties expected for the light and heavy actinides. It is believed that the unusual aspects of the bonding in bulk Pu are apt to be enhanced at a surface or in a thin layer of Pu adsorbed on a substrate, as a result of the reduced atomic coordination of a surface atom and the narrow bandwidth of surface states. For this reason, Pu surfaces and films may provide a valuable source of information about bonding in Pu, since the initial crossover from delocalized to localized behavior probably takes place at the Pu surface. For theoretical studies of surfaces, it is common practice to model the surface of a semi-infinite solid by an ultra-thin film (UTF), thin enough to be treated with high-precision density functional calculations, but thick enough to model the intended surface realistically. Determination of an appropriate UTF thickness is complicated by the existence of possible quantum oscillations in UTF properties as a function of thickness; the so-called quantum size effect (QSE). These oscillations were first predicted by calculations on jellium films [11,12] and were subsequently confirmed by band structure calculations on free-standing UTFs composed of discrete atoms [13–16]. The adequacy of the UTF approximation obviously depends on the size of any QSE in the relevant properties of the model film. Thus, it is important to determine the magnitude of the QSE in a

[a] e-mail: akr@uta.edu

given UTF prior to using that UTF as a model for the surface. This is particularly important for Pu films, since the strength of the QSE is expected to increase with the number of valence electrons.

In the present study, UTFs of fcc Pu $\delta$-phase, instead of $\alpha$-phase, are selected for investigation, based on the following considerations. First, $\delta$-Pu is technologically more important than $\alpha$-Pu. Known to be monoclinic with sixteen atoms per unit cell, the ambient ground-state $\alpha$-phase is very brittle and not suitable for engineering applications, whereas Pu $\delta$-phase is more ductile and useful in practice. Also, although the monoclinic $\alpha$-phase of plutonium is more stable under ambient conditions, there are advantages to studying $\delta$-like layers. First, a very small amount of impurities can stabilize $\delta$-Pu at room temperature. For example, $Pu_{1-x}Ga_x$ has the fcc structure and physical properties of $\delta$-Pu for $0.020 \leq x \leq 0.085$ [17]. Second, grazing-incidence photoemission studies combined with the calculations of Eriksson et al. [18] suggest the existence of a small-moment $\delta$-like surface on $\alpha$-Pu. Theoretical work on plutonium monolayer has also indicated the possibility of such a surface [19]. Photoemission results by Arko et al. indicate that both $\alpha$- and $\delta$-phases of Pu display a narrow, temperature-independent, $5f$-related feature at the Fermi energy, narrower in $\delta$-Pu than in $\alpha$-Pu, suggestive of possible heavy-fermion-like behavior [20]. Recently, high-purity ultra-thin layers of plutonium deposited on Mg were studied by X-ray photoelectron (XPS) and high-resolution valence band (UPS) spectroscopy by Gouder et al. [21]. They found that the degree of delocalization of the $5f$ states depends in a very dramatic way on the layer thickness and the itinerant character of the $5f$ states is gradually lost with reduced thickness, suggesting that the thinner films are $\delta$-like. At intermediate thickness, three narrow peaks appear close to the Fermi level and a comparative study of bulk $\alpha$-Pu indicated a surface reorganization yielding more localized $f$-electrons at thermodynamic equilibrium. Also, $\delta$-plutonium shows negative thermal expansion coefficient and exhibits superconductivity alloyed with other elements. Finally, it may be possible to study $5f$ localization in plutonium through adsorptions on carefully selected substrates for which the adsorbed layers are more likely to be $\delta$-like than $\alpha$-like.

Regarding $\delta$-Pu surface, there are *very few* theoretical calculations in the literature. Using the self-consistent film-linearized muffin-tin-orbital (FLMTO) method, Hao et al. studied the electronic structures of the (100) and (111) surfaces using five-layer slab geometries [18]. The calculated work functions for the systems were found to be 3.68 eV and 4.14 eV, respectively, with the $6p$ electrons treated as core states. They obtained a much higher value of 8.4 eV, if the $6p$ electrons were treated as valence electrons. Ray and Boettger used linear combinations of Gaussian-type orbitals-fitting function (LCGTO-*FF*) method to study $\delta$-Pu (001) and (111) films up to five layers. Because of highly compute-intensive nature of this method, spin-polarization was not included in these calculations beyond the di-layer. They found that the surface energies converged within the first three layers, while the work function exhibited a strong QSE [22]. Using the full-potential linearized-augmented-plane-wave (FP-LAPW) method, Wu and Ray [23] have investigated bulk $\delta$-Pu and the (001) surface up to seven layers at the non-spin-polarized-no-spin-orbit-coupling (NSP-NSO), non-spin-polarized–spin-orbit-coupling (NSP-SO), spin-polarized-no-spin-orbit-coupling (SP-NSO), spin-polarized-spin-polarized-coupling (SP-SO) levels of theory. The surface energy was again found to be rapidly converged at all four levels of theory and the semi-infinite surface energy was predicted to be 0.692 eV at the SP-SO level of theory. Recently, using the FP-LAPW method, we have studied bulk $\delta$-Pu at the antiferromagnetic-no-spin-orbit-coupling (AFM-NSO) and antiferromagnetic-spin-orbit-coupling (AFM-SO) levels of theory and the electronic structures of $\delta$-Pu (111) surface up to seven layers at the non-spin-polarized-no-spin-orbit coupling (NSP-NSO), non-spin-polarized-spin-orbit coupling (NSP-SO), spin-polarized-no-spin-orbit coupling (SP-NSO), spin-polarized-spin-orbit coupling (NSP-NSO), antiferromagnetic-no-spin-orbit coupling (AFM-NSO), and antiferromagnetic-spin-orbit-coupling (AFM-SO) levels of theory [24]. This paper is a natural extension of the above study for the other high symmetry face, namely the (110) surface of $\delta$-Pu. The (110) surface is more open with the density of atoms being lower than the corresponding densities of the (001) and (111) surfaces. The optimized lattice constants of bulk $\delta$-Pu as derived in the previous studies [23,24] and as shown in Table 1, are used in the present study. Because of *severe* demands on computational resources due to the large system sizes involved, no surface relaxations and/or reconstructions have been taken into account. It is neither expected nor believed that the Pu surface undergoes any significant relaxations and/or reconstructions. However, the qualitative and the quantitative trends in the results reported below should hold true in any future detailed investigations taking into account surface relaxations and/or reconstructions.

**Table 1.** Lattice constants $a$ (a.u.), bulk modulus $B$ (GPa), and magnetic moments $MM$ ($\mu_B$/atom) of bulk$\delta$-Pu.

| | Theory | $A$ (a.u.) | $B$ (GPa) | $MM$ ($\mu_B$/atom) |
|---|---|---|---|---|
| Ref. 23 | NSP-NSO | 7.89 | 214.2 | |
| | NSP-SO | 8.10 | 101.9 | |
| | SP-NSO | 9.10 | 32.5 | 5.8 |
| | SP-SO | 8.93 | 24.9 | 5.2 |
| Ref. 24 | AFM-NSO | 8.60 | 37.4 | 0 |
| | AFM-SO | 8.66 | 32.8 | 0 |
| Experiment | | 8.76[a] | 30–35[b] | 0 |

[a]Reference [25]; [b]reference [26].

## 2 Computational method

As in our previous works [23,24], the computations have been carried out using the full-potential all-electron method with mixed basis APW+lo/LAPW

method as implemented in the WIEN2k suite of programs [27]. The generalized-gradient-approximation to density functional theory (GGA-DFT) [28] with a gradient corrected Perdew-Berke-Ernzerhof (PBE) exchange-correlation functional [29] is used and the Brillouin-zone integrations are conducted by an improved tetrahedron method of Blöchl-Jepsen-Andersen [30]. In the WIEN2k code, the alternative basis set APW+lo is used inside the atomic spheres for the chemically important orbitals that are difficult to converge, whereas LAPW is used for others. The local orbitals scheme leads to significantly smaller basis sets and the corresponding reductions in computing time, given that the overall scaling of LAPW and APW + lo is given by $N^3$, where $N$ is the number of atoms. Also, results obtained with the APW + lo basis set converge much faster and often more systematically towards the final value [31]. As far as relativistic effects are concerned, core states are treated fully relativistically in WIEN2k and for valence states, two levels of treatments are implemented: (1) a scalar relativistic scheme that describes the main contraction or expansion of various orbitals due to the mass-velocity correction and the Darwin s-shift [32] and (2) a fully relativistic scheme with spin-orbit coupling included in a second-variational treatment using the scalar-relativistic eigen functions as basis [33,34]. Our computations have been carried out at both scalar-relativistic and fully-relativistic levels to determine the effects of relativity. To calculate the total energy at 0 K, a constant muffin-tin radius ($R_{\rm mt}$) of 2.70 a.u. is used for all atomic volumes. The plane-wave cut-off $K_{\rm cut}$ is determined by $R_{\rm mt}K_{\rm cut} = 9.0$. The (110) surface of fcc $\delta$-Pu is modeled by periodically repeated slabs of N Pu layers (with one atom per layer and $N$ = 1–7) separated by a 60 Bohr a.u. vacuum gap. Twenty-four irreducible K points have been used for reciprocal-space integrations. For each calculation, the energy convergence criterion is set to be 0.001 mRy. In the AFM calculations, the atomic spin moments are aligned in (001) ferromagnetic sheets with adjacent sheets having anti-parallel spins and spin quantization along the [001] direction, as this kind of setting has been shown to produce lower energy [35].

## 3 Results and discussions

### 3.1 Energetics

Figure 1 shows the total energies for the $\delta$-Pu (110) films at six theoretical levels, namely, NSP-NSO, NSP-SO, SP-NSO, SP-SO, AFM-NSO, and AFM-SO, respectively. For the sake of comparison, the total energies of the corresponding bulk $\delta$-Pu are also plotted in Figure 1. Three features are evident: a) the $\delta$-Pu (110) films at the six theoretical levels all have higher total energies than the corresponding bulk, implying that $\delta$-Pu (110) films are less stable than $\delta$-Pu bulk; b) the total energies of the films decrease with an increase in the number of the layers, and the slope of decrease gradually approaches zero as the number of Pu layers increase; c) the descending sequence of the total energy is as follows: NSP-NSO → SP-NSO → AFM-NSO → NSP-SO → SP-SO → AFM-SO. It follows that both spin-polarization and spin-orbit coupling effects have important influences on lowering the total energies of the $\delta$-Pu (110) films. From the energetics point of view, the AFM-SO level of theory provides the ground state of the $\delta$-Pu (110) films, as it has the lowest total energy and are more stable than other levels, while the $\delta$-Pu (110) films without spin-orbit coupling effects included have higher total energies.

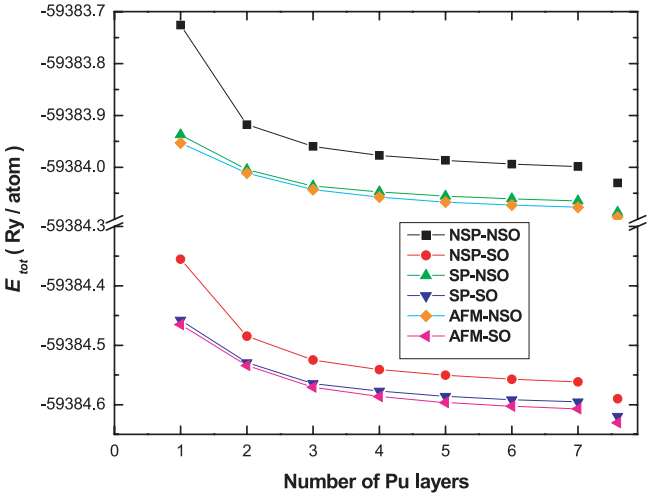


**Fig. 1.** Total energies $E_{tot}$ (Ry/atom) of $\delta$-Pu (110) films for different layers ($n$ = 1–7). For comparison, the corresponding total energies of $\delta$-Pu bulks are also plotted at the farthest right of the figure.

In Table 2, we have shown the cohesive energies $E_{\rm coh}$ (eV/atom) with respect to the monolayer, the incremental energies $E_{\rm inc}$ (eV) of $n$-layers with respect to $(n-1)$-layers plus a monolayer, and the surface energies $E_s$ (J/m$^2$) for the $\delta$-Pu (110) films up to seven layers at the six different levels of theory. The cohesive energies and the incremental energies are also plotted in Figures 2 and 3, respectively. We note that the cohesive energies increase monotonously with the number of layers at all six levels of calculations, while the incremental energies become relatively stable when the number of layers is greater than five. The above features are in good agreement with our previous full-potential-linearized-augmented-plane-wave (FPLAPW) results for the $\delta$-Pu (001) films at four levels (NSP-NSO, NSP-SO, SP-NSO, and SP-SO) of theory [23], as well as with the results for the $\delta$-Pu (111) films up to seven layers at the NSP-NSO, NSP-SO, SP-NSO, SP-SO, AFM-NSO, and AFM-SO levels [24].

The surface energy $E_s$ may be estimated from an $n$-layer calculation as [36]

$$E_s = (1/2)[E_{tot}(n) - nE_B], \qquad (1)$$

where $E_{tot}(n)$ is the total energy of the $n$-layer film and $E_B$ is the total energy of the infinite crystal. If $n$ is sufficiently large and $E_{tot}(n)$ as well as $E_B$ are known to infinite precision, equation (1) is exact. If, however, the bulk and the film calculations are not entirely consistent

**Table 2.** Calculated energies of $\delta$-Pu (110) films for different layers ($n$ = 1–7). $E_{coh}$ is the cohesive energy (eV/atom) with respect to monolayer; $E_{inc}$ is incremental energy (eV) of $n$-layers with respect to $(n-1)$-layers plus a monolayer; $E_s$ is surface energies (J/m$^2$).

| $n$ | Theory | $E_{coh}$ (eV/atom) | $E_{inc}$ (eV) | $E_s$ (J/m$^2$) |
|---|---|---|---|---|
| 1 | NSP-NSO | | | 2.67 |
| | NSP-SO | | | 1.96 |
| | SP-NSO | | | 0.99 |
| | SP-SO | | | 1.11 |
| | AFM-NSO | | | 1.11 |
| | AFM-SO | | | 1.24 |
| 2 | NSP-NSO | 2.61 | 5.21 | 1.94 |
| | NSP-SO | 1.76 | 3.53 | 1.75 |
| | SP-NSO | 0.91 | 1.82 | 1.09 |
| | SP-SO | 0.98 | 1.96 | 1.23 |
| | AFM-NSO | 0.79 | 1.57 | 1.36 |
| | AFM-SO | 0.93 | 1.87 | 1.48 |
| 3 | NSP-NSO | 3.17 | 4.31 | 1.81 |
| | NSP-SO | 2.30 | 3.39 | 1.63 |
| | SP-NSO | 1.34 | 2.19 | 1.00 |
| | SP-SO | 1.46 | 2.42 | 1.12 |
| | AFM-NSO | 1.22 | 2.10 | 1.32 |
| | AFM-SO | 1.43 | 2.42 | 1.41 |
| 4 | NSP-NSO | 3.41 | 4.13 | 1.79 |
| | NSP-SO | 2.53 | 3.19 | 1.63 |
| | SP-NSO | 1.49 | 1.96 | 1.03 |
| | SP-SO | 1.63 | 2.14 | 1.14 |
| | AFM-NSO | 1.42 | 2.00 | 1.34 |
| | AFM-SO | 1.65 | 2.30 | 1.41 |
| 5 | NSP-NSO | 3.54 | 4.05 | 1.82 |
| | NSP-SO | 2.65 | 3.17 | 1.64 |
| | SP-NSO | 1.60 | 2.04 | 1.02 |
| | SP-SO | 1.75 | 2.23 | 1.12 |
| | AFM-NSO | 1.55 | 2.07 | 1.31 |
| | AFM-SO | 1.78 | 2.33 | 1.40 |
| 6 | NSP-NSO | 3.64 | 4.14 | 1.80 |
| | NSP-SO | 2.75 | 3.20 | 1.63 |
| | SP-NSO | 1.68 | 2.04 | 1.01 |
| | SP-SO | 1.82 | 2.19 | 1.12 |
| | AFM-NSO | 1.63 | 2.02 | 1.32 |
| | AFM-SO | 1.87 | 2.29 | 1.41 |
| 7 | NSP-NSO | 3.70 | 4.09 | 1.80 |
| | NSP-SO | 2.81 | 3.18 | 1.63 |
| | SP-NSO | 1.73 | 2.07 | 0.99 |
| | SP-SO | 1.88 | 2.20 | 1.12 |
| | AFM-NSO | 1.68 | 2.01 | 1.33 |
| | AFM-SO | 1.93 | 2.27 | 1.42 |

with each other, $E_s$ will diverge linearly with increasing $n$ [37]. Stable and internally consistent estimates of $E_s$ and $E_B$ can, however, be extracted from a series of values of $E_{tot}(n)$ via a linear least-squares fit to [36]

$$E_{tot}(n) = E_B n + 2E_s. \quad (2)$$

To obtain an optimal result, the fit to equation (2) should only be applied to films which include, at least, one bulk-like layer, i.e., $n > 2$. We have independently applied this fitting procedure to the $\delta$-Pu (110) films

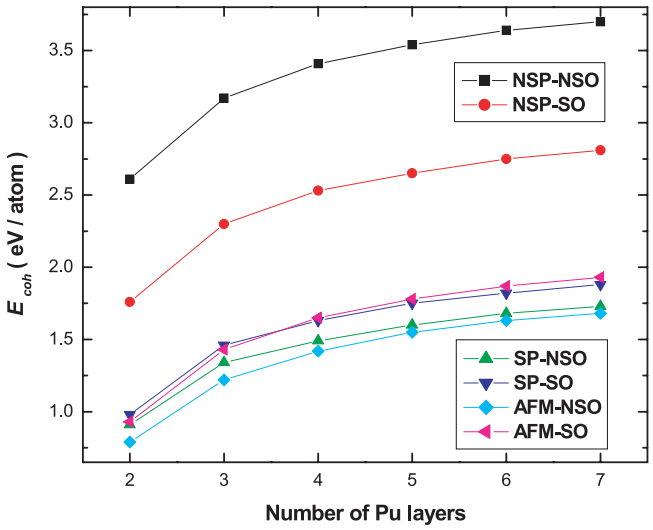


**Fig. 2.** Cohesive energies $E_{coh}$ (eV/atom) with respect to monolayer for$\delta$-Pu (110) films for different layers ($n$ = 2–7).

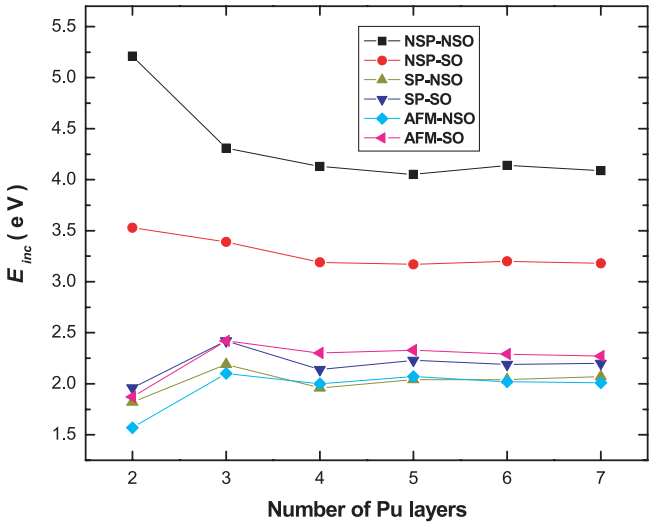


**Fig. 3.** Incremental energies $E_{inc}$ (eV) of $\delta$-Pu (110) $n$-layers with respect to ($n$-1)-layers plus the monolayer.

at all six levels of theory, respectively. Accordingly, six values of$E_B$, i.e., –59384.027708, –59384.589475, –59384.086243, –59384.618469, –59384.102394, and –59384.634719 Ry/atom, and six values of semi-infinite surface energy $E_s$, i.e., 1.80, 1.63, 1.01, 1.12, 1.33, and 1.41 J/m$^2$, are derived for the $\delta$-Pu (110) films at the NSP-NSO, NSP-SO, SP-NSO, SP-SO, AFM-NSO, and AFM-SO levels, respectively. Thus, the semi-infinite surface energy decreases by close to twenty-two percent from the NSP-NSO level to the AFM-SO level. The surface energy for each layer has been computed using the calculated $n$-layer total energy and appropriate fitted bulk energy. The calculated results are listed in Table 2 and plotted in Figure 4. Several characteristics of the surface energies are evident from the above results. First, for all the six theoretical levels, the surface energy of $\delta$-Pu (110) films pretty well converges to the corresponding

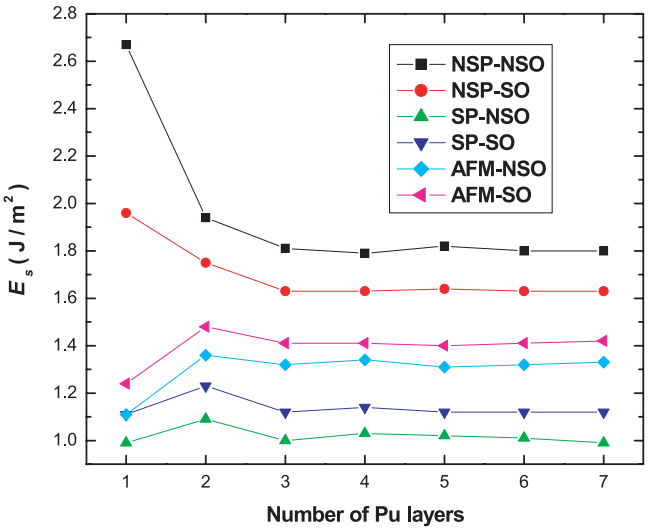


**Fig. 4.** Surface energies $E_s$ (J/m$^2$) for$\delta$-Pu (110) films for different layers ($n$ = 1–7).

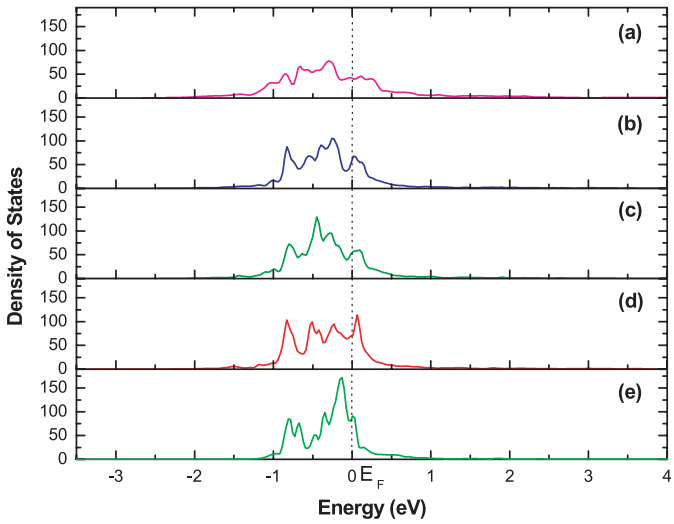


**Fig. 5.** Density of states of $5f$ electrons in (a)$\delta$-Pu bulk (e) 1-layer at the AFM-SO levels, respectively.

semi-infinite surface energy when the number of layers reaches three, which matches well with the observations in reference [22] for $\delta$-Pu (111) and (001) films up to five layers using the linear combinations of Gaussian orbitals – fitting function (LCGTO-FF) method and in reference [23] for $\delta$-Pu (001) films up to seven layers, as well as in reference [24] for $\delta$-Pu (111) films up to seven layers using the FP-LAPW method. This further confirms our previous observation [22–24] that a 3-layer film may be sufficient for future atomic and molecular adsorption studies on Pu films, if the primary quantity of interest is the chemisorption energy. Second, the semi-infinite surface energy for $\delta$-Pu (110) film at the AFM-SO level are calculated to be 1.41 J/m$^2$, which is higher than the corresponding value of 1.16 J/m$^2$ for the $\delta$-Pu (111) film [24]. It should be pointed out that this observation regarding the sequence of surface energy is consistent with the stability of these two surfaces, i.e., the $\delta$-Pu (111) surface is more stable than the $\delta$-Pu (110) surface. Finally, the density of states and the band structure of $\delta$-Pu (110) films are shown in Figures 5 and 6, respectively.

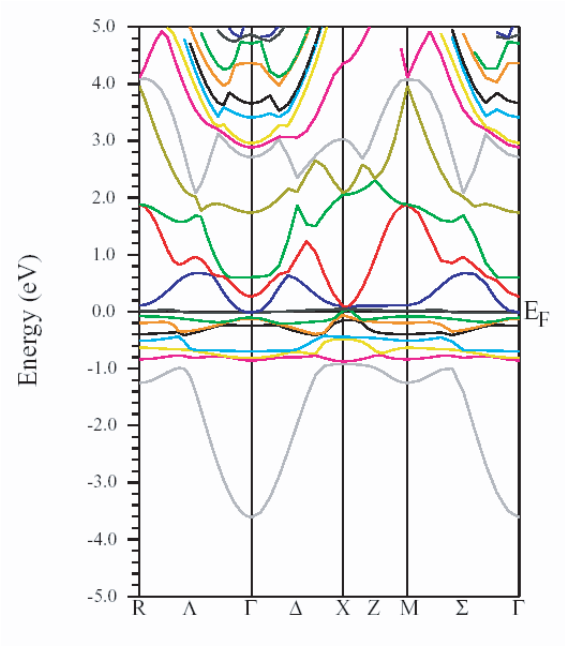


**Fig. 6.** Band structure of $\delta$-Pu (110) film with 7-layer at the AFM-SO level.

### 3.2 Magnetic properties

The issue of magnetic properties of $\delta$-Pu has been a subject of controversy for many years, as none of the experiments so far provides any evidence for either ordered or disordered magnetic moments in $\delta$-Pu [38] while considerable magnetic moments are predicted by various researchers through some modern DFT calculations [35,39,40]. It should be pointed out that for the commonly believed ground state (AFM) of $\delta$-Pu there are also some discrepancy among theoretical calculations regarding magnetic properties of bulk $\delta$-Pu, e.g., a magnetic moment of 1.5–4.6 $\mu_B$/atom was predicted by some researchers [35,39,40], while a null magnetic moment was noted by other researchers [24,41]. As for the magnetic properties of $\delta$-Pu films, however, there are no experimental results available in the literature and hopefully, our theoretical results as detailed below will stimulate experimental study.

Accordingly, the magnetic moments of $\delta$-Pu (110) films are calculated, respectively, at the SP-NSO, SP-SO, AFM-NSO, and AFM-SO levels, and the results are listed in Table 3 as well as plotted in Figure 7. For comparison, the corresponding magnetic moments of bulk $\delta$-Pu are also shown in Figure 7. Several features can be seen from these results. First, for the $\delta$-Pu (110) films at the AFM-NSO and AFM-SO levels, the magnetic moments show a

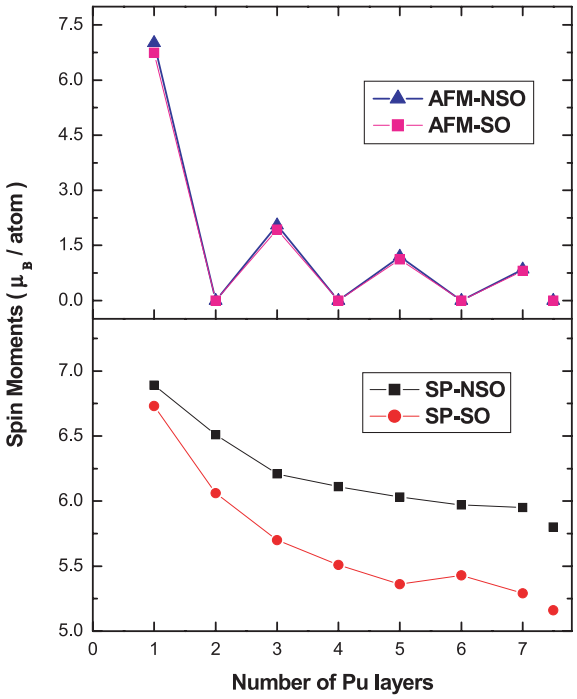


**Fig. 7.** Spin moments ($\mu_B$/atom) of $\delta$-Pu (110) films for different layers ($n$ = 1–7). For comparison, the corresponding spin moments of $\delta$-Pu bulks are also plotted at the farthest right of the figure.

behavior of oscillation, which becomes smaller with the increase of the number of layers, and gradually the magnetic moments approach the bulk value of zero. The $\delta$-Pu (110) films with an odd number of layer have magnetic moments decreasing with the increase of the number of layers, while the $\delta$-Pu (110) films with an even number of layer always have zero magnetic moments, the same as that of $\delta$-Pu bulk. Second, for the $\delta$-Pu (110) films at the SP-NSO and SP-SO levels, the magnetic moments are larger than the corresponding bulk values of 5.8 and 5.2 $\mu_B$/atom, and with the increase of the number of layers the magnetic moments gradually approach the values of the corresponding bulks. Third, for the $\delta$-Pu (110) films at the anti-ferromagnetic state, spin-orbit coupling has negligible effect on the magnetic properties while for the $\delta$-Pu (110) films at the spin-polarized state, spin-orbit coupling lowers the magnetic moments.

We also calculated spin-polarization energies and spin-orbit coupling energies for the $\delta$-Pu (110) films at various theoretical levels, and the results are shown in Table 3 as well as in Figure 8. We note that convergence is achieved rather quickly at all levels when the number of the layers equals three. It can also be seen that spin-orbit coupling effect plays a more important role than spin-polarization in reducing the total energies of the $\delta$-Pu (110) films, i.e., spin-orbit coupling effect reduces the total energy by 7.21–7.66 eV/atom, while spin-polarization effect decreases the total energy by only 0.46–1.06 eV/atom. These results are in excellent agreement with our previous results for the (111) and (001) surfaces [24], indicating

**Table 3.** Spin magnetic moments $\mu_s$ ($\mu_B$/atom), spin-polarization energies $E_{sp}$ (eV/atom), spin-orbit coupling energies $E_{so}$ (eV/atom), and work functions $W$ (eV) for $\delta$-Pu (110) films with different layers ($n$ = 1–7).

| $N$ | Theory | $\mu_s$ ($\mu_B$/atom) | $E_{sp}$ (eV/atom) | $E_{so}$ (eV/atom) | $W$ (eV) |
|---|---|---|---|---|---|
| 1 | NSP-NSO | | | | 2.96 |
| | NSP-SO | | | 8.56 | 2.99 |
| | SP-NSO | 6.89 | 2.88 | | 2.83 |
| | SP-SO | 6.73 | 1.39 | 7.07 | 2.88 |
| | AFM-NSO | 7.01 | 3.08 | | 2.85 |
| | AFM-SO | 6.74 | 1.45 | 5.97 | 2.91 |
| 2 | NSP-NSO | | | | 3.13 |
| | NSP-SO | | | 7.71 | 3.12 |
| | SP-NSO | 6.51 | 1.18 | | 2.77 |
| | SP-SO | 6.06 | 0.60 | 7.14 | 2.92 |
| | AFM-NSO | 0 | 1.27 | | 2.83 |
| | AFM-SO | 0 | 0.67 | 7.11 | 2.93 |
| 3 | NSP-NSO | | | | 3.35 |
| | NSP-SO | | | 7.69 | 3.26 |
| | SP-NSO | 6.21 | 1.04 | | 3.04 |
| | SP-SO | 5.70 | 0.54 | 7.19 | 3.02 |
| | AFM-NSO | 2.05 | 1.14 | | 3.10 |
| | AFM-SO | 1.93 | 0.62 | 7.17 | 3.08 |
| 4 | NSP-NSO | | | | 3.29 |
| | NSP-SO | | | 7.67 | 3.23 |
| | SP-NSO | 6.11 | 0.95 | | 2.87 |
| | SP-SO | 5.51 | 0.49 | 7.21 | 3.14 |
| | AFM-NSO | 0 | 1.09 | | 2.99 |
| | AFM-SO | 0 | 0.62 | 7.20 | 2.95 |
| 5 | NSP-NSO | | | | 3.13 |
| | NSP-SO | | | 7.67 | 3.18 |
| | SP-NSO | 6.03 | 0.94 | | 2.86 |
| | SP-SO | 5.36 | 0.48 | 7.22 | 3.08 |
| | AFM-NSO | 1.20 | 1.10 | | 2.99 |
| | AFM-SO | 1.12 | 0.63 | 7.20 | 3.00 |
| 6 | NSP-NSO | | | | 3.22 |
| | NSP-SO | | | 7.66 | 3.26 |
| | SP-NSO | 5.97 | 0.91 | | 2.84 |
| | SP-SO | 5.43 | 0.47 | 7.22 | 3.02 |
| | AFM-NSO | 0 | 1.07 | | 2.90 |
| | AFM-SO | 0 | 0.62 | 7.21 | 2.95 |
| 7 | NSP-NSO | | | | 3.15 |
| | NSP-SO | | | 7.66 | 3.19 |
| | SP-NSO | 5.95 | 0.90 | | 2.86 |
| | SP-SO | 5.29 | 0.46 | 7.21 | 3.02 |
| | AFM-NSO | 0.85 | 1.06 | | 2.97 |
| | AFM-SO | 0.81 | 0.62 | 7.21 | 2.99 |

that crystalline planes have little effects on the values of spin-polarization energies and spin-orbit coupling energies of $\delta$-Pu.

### 3.3 Work functions

As stated in the introduction, one major objective of the present study is to investigate the quantum size effect (QSE) in $\delta$-Pu (110) films. It is commonly believed that surface energy and work function are two parameters

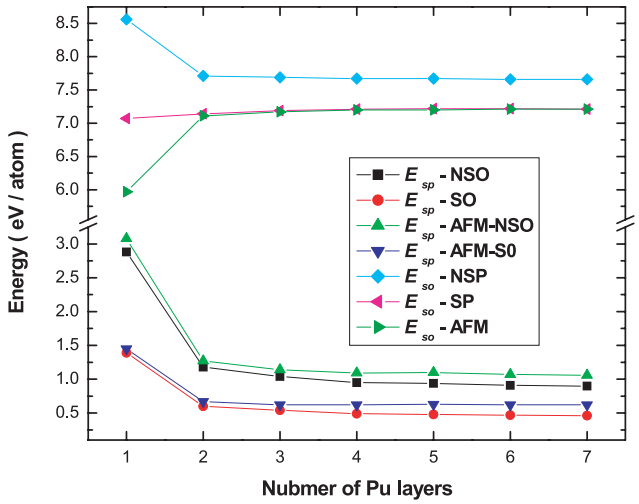


**Fig. 8.** Spin-polarization energies $E_{sp}$ (eV/atom) and spin-orbit coupling energies $E_{so}$ (eV/atom) of $\delta$-Pu (110) films for different layers ($n = 1$–7).

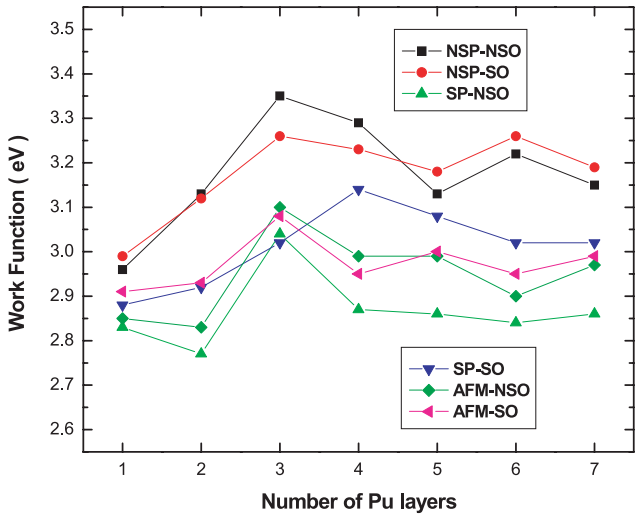


**Fig. 9.** 9 Work functions (eV) of$\delta$-Pu (110) films for different layers ($n = 1$–7).

which are sensitive to QSE [11,12,16]. As shown above, the surface energy in $\delta$-Pu (110) films quickly converges when the number of layers reaches three and therefore there is no apparently strong QSE regarding the surface energy in $\delta$-Pu (110) films.

As far as work function $W$ is concerned, we have calculated $W$according to the following formula

$$W = V_0 - E_F, \tag{3}$$

where $V_0$ is the Coulomb potential energy at the half height of the slab including the vacuum layer and $E_F$ is the Fermi energy. Accordingly, the work functions of $\delta$-Pu (110) films up to seven layers are calculated at the six theoretical levels, i.e., NSP-NSO, NSP-SO, SP-NSO, SP-SO, AFM-NSO, and AFM-SO, respectively, and the results are listed in Table 3 as well as plotted in Figure 9. From these results, several features can be observed. First, strong oscillations are present in the values of the work function, indicating that QSE can be pronounced for $\delta$-Pu (110) films up to seven layers and possibly beyond at all six theoretical levels, including the ground state (AFM-SO).. This implies that for the $\delta$-Pu (110) surface, film thickness greater than $n = 7$ will be required for any chemisorption investigation that requires an accurate prediction of the adsorbate-inducted work function shift. We note that this observation for $\delta$-Pu (110) surface is quite different from our previous observation for $\delta$-Pu (111) surface [24], where we found that a 5-layer film of $\delta$-Pu (111) may be sufficient for any future adsorption investigation that requires an accurate prediction of adsorbate-induced work function shift. Second, the work functions in $\delta$-Pu (110) films are smaller than the corresponding values in $\delta$-Pu (111) films [24]. This observation regarding the sequence of work functions is reasonable as it is consistent with the surface stability, i.e., the $\delta$-Pu (111) surface is more stable with lower total energy and therefore more energy is needed to move the electron far from the (111) surface than that in the (110) surface. Third, the work functions for $\delta$-Pu (110) films with 7-layers are calculated to be 3.15, 3.19, 2.86, 3.02, 2.97, and 2.99 eV at the NSP-NSO, NSP-SO, SP-NSO, SP-SO, AFM-NSO, and AFM-SO, respectively,. Recently, Durakiewicz et al. measured the work function of $\delta$-Pu for various degrees of surface oxidation and based on their measurement a preliminary estimate of 3.1–3.3 eV is obtained for the work function of a clean polycrystalline sample of $\delta$-Pu [42]. It should be noted that our calculated values of work functions for $\delta$-Pu (110) films are in good agreement with this estimated experimental value.

## 4 Conclusions

Full-potential-linearized-augmented-plane-wave calculations show that the antiferromagnetic state with spin-orbit coupling effects is the ground state of $\delta$-Pu (110) films. For the $\delta$-Pu (110) films, the total energy decreases with the increase of the number of layers, and when the number of layers reaches three the surface energy quickly converges to the value of 1.41 J/m$^2$ at the ground state (AFM-SO).

For the $\delta$-Pu (110) films at the AFM-NSO and AFM-SO levels, the magnetic moments show a behavior of oscillation, which becomes smaller with the increase in the number of layers, and gradually the magnetic moments approach the bulk value of zero. Spin-orbit coupling effects can reduce the energy of $\delta$-Pu (110) films by 7.21–7.66 eV/atom, while spin-polarization effect decreases the energy only by 0.46–1.06 eV/atom. It is also found that the work function shows a strong quantum size effect for $\delta$-Pu (110) films up to seven layers and possibly beyond and the work function of $\delta$-Pu (110) films at the ground state is predicted to be around 2.99 eV.

This work is supported by the Chemical Sciences, Geosciences and Biosciences Division, Office of Basic Energy Sciences, Office of Science, U.S. Department of Energy (Grant No. DE-FG02-03ER15409) and the Welch Foundation, Houston, Texas (Grant No. Y-1525).

## References


1. J.J. Katz, G.T. Seaborg, L.R. Morss, *The Chemistry of the Actinide Elements* (Chapman and Hall, 1986)
2. *Transuranium Elements: A Half Century*, edited by L.R. Morss, J. Fuger, (American Chemical Society, Washington, D.C., 1992)
3. L.R. Morss, Mat. Res. Soc. Symp. Proc. **802**, DD 4.1.1 (2004).
4. *Chemistry of the Actinide and Transactinide Elements*, edited by J.J. Katz, L.R. Morss, J. Fuger, N.M. Edelstein (Springer-Verlag, New York, in press)
5. *Plutonium Futures – The Science*, edited by K.K.S. Pillay, K.C. Kim, American Institute of Physics Conference Proceedings, **532** (2000)
6. *Plutonium Futures – The Science*, edited by G.D. Jarvinen, American Institute of Physics Conference Proceedings, **673** (2003)
7. A.M. Boring, J.L. Smith, *Plutonium Condensed-Matter Physics: A Survey of Theory and Experiment,* in *Challenges in Plutonium Science*, Los Alamos Science **1**, 90 (2000)
8. *Advances in Plutonium Chemistry 1967-2000*, edited by D. Hoffman (American Nuclear Society, La Grange, Illinois and University Research Alliance, Amarillo, Texas, 2002)
9. *Proceedings of the Materials Research Society*, edited by, L. Soderholm, J.J. Joyce, M.F. Nicol, D.K. Shuh, J.G. Tobin **802**, (2004)
10. S.Y. Savrasov, G. Kotliar, E. Abrahams, Nature **410**, 793 (2001); X. Dai, S.Y. Savrasov, G. Kotliar, A. Migliori, H. Ledbetter, E. Abrahams, Science **300**, 953 (2003); J. Wong, M. Krisch, D.L. Farber, F. Occelli, A.J. Schwartz, T.-C. Chiang, M. Wall, C. Boro, R. Xu, Science **301,** 1078 (2003); P. Söderlind, B. Sadigh, Phys. Rev. Lett. **92**, 185702 (2004); P. Söderlind, O. Eriksson, B. Johansson, J.M. Wills, Phys. Rev. B **55**, 1997 (1997); B. Sadigh, P. Söderlind, W.G. Wolfer, Phys. Rev. B **68**, 241101(R) (2003)
11. E.K. Schulte, Surf. Sci. **55**, 427 (1976)
12. P.J. Feibelman, Phys. Rev. B **27**, 1991 (1982)
13. E.E. Mola, J.L. Vicente, J. Chem. Phys. **84**, 2876 (1986)
14. I.P. Batra, S. Ciraci, G.P. Srivastava, J.S. Nelson, C.Y. Fong, Phys. Rev. B **34**, 8246 (1986)
15. J.C. Boettger, S.B. Trickey, Phys. Rev. B **45**, 1363 (1992); J.C. Boettger, Phys. Rev. B **53**, 13133 (1996)
16. C.M. Wei, M.Y. Chou, Phys. Rev. B **66**, 233408 (2002)
17. N.J. Curro, L. Morales, Mat. Res. Soc. Symp. Proc. **802**, DD2.4.1 (2004)
18. O. Eriksson, L.E. Cox, B.R. Cooper, J.M. Wills, G.W. Fernando, Y.-G. Hao, A.M. Boring, Phys. Rev. B **46**, 13576 (1992); Y.-G. Hao, G.W. Fernando, B.R. Cooper, J. Vac. Sci. Tech. A **7**, 2065 (1989); Y.-G. Hao, O. Eriksson, G.W. Fernando, B.R. Cooper, Phys. Rev. B **43**, 9467 (1991); L.E. Cox, O. Eriksson, B.R. Cooper, Phys. Rev. B **46**, 13571 (1992)s
19. A.K. Ray, J.C. Boettger, Eur. Phys. J. B **27**, 429 (2002)
20. A.J. Arko, J.J. Joyce, L. Morales, J. Wills, J. Lashley, F. Wastin, J. Rebizant, Phys. Rev. B **62**, 1773 (2000)
21. T. Gouder, L. Havela, F. Wastin, J. Rebizant, Europhys. Lett. **55**, 705 (2001); L. Havela, T. Gouder, F. Wastin, J. Rebizant, Phys. Rev. B **65**, 235118 (2002). T. Gouder, J. Alloys. Comp. **271–273**, 841 (1998); J. El. Spec. Rel. Phenom. **101–103**, 419 (1999)
22. A.K. Ray, J.C. Boettger, Phys. Rev. B **70**, 085418 (2004); J.C. Boettger, A.K. Ray, Int. J. Quant. Chem., in press
23. X. Wu, A.K. Ray, Phys. Rev. B, **72,** 045115 (2005) and references therein
24. H.R. Gong, A.K. Ray, submitted for publication
25. F.H. Ellinger, Trans. Am. Inst. Min. Metall. Pet. Eng. **206**, 1256 (1956)
26. R.L. Moment, in *Plutonium and Other Actinides*, edited by H. Blank, R. Lindner (North-Holland, Amsterdam, 1976), p. 687
27. P. Blaha, K. Schwarz, G.K.H. Madsen, D. Kvasnicka, J. Luitz, *WIEN2k*, An Augmented Plane Wave + Local Orbitals Program for Calculating Crystal Properties (Tech. Univ. Wien, Austria, 2001); P. Blaha, K. Schwarz, P.I. Sorantin, S.B. Trickey, Comp. Phys. Comm. **59**, 399 (1990); M. Petersen, F. Wagner, L. Hufnagel, M. Scheffler, P. Blaha, K. Schwarz, Comp. Phys. Comm. **126**, 294 (2000); K. Schwarz, P. Blaha, G.K.H. Madsen, Comp. Phys. Comm. **147**, 71 (2002)
28. P. Hohenberg, W. Kohn, Phys. Rev. B **136**, 864 (1964); W. Kohn, L.J. Sham, Phys. Rev. A **140**, 1133 (1965); *Density Functional Theory for Many Fermion Systems*, edited by S.B. Trickey (Academic, San Diego, 1990); R.M. Dreialer, E.K.U. Gross, *Density Functional Theory: An Approach to Quantum Many Body Problem* (Springer, Berlin, 1990); *Electronic Density Functional Theory Recent Progress and New Directions*, edited by J.F. Dobson, G. Vignale, M.P. Das (Plenum, New York, 1998)
29. J.P. Perdew in *Electronic Structure of Solids,* edited by Ziesche, H. Eschrig (Akademie Verlag, Berlin, 1991), p. 11; J.P. Perdew, K. Burke, Y. Wang, Phys. Rev. B **54**, 16533 (1996); J.P. Perdew, K. Burke, M. Ernzerhof, Phys. Rev. Lett. **77**, 3865 (1996)
30. P.E. Blöchl, O. Jepsen, O.K. Andersen, Phys. Rev. B **49**, 16223 (1994)
31. G.K.H. Madsen, P. Blaha, K. Schwarz, E. Sjostedt, L. Nordstrom, Phys. Rev. B **64**, 195134 (2001)
32. D.D. Koelling, B.N. Harmon, J. Phys. C: Sol. St. Phys. **10**, 3107 (1977)
33. A.H. MacDonnald, W.E. Picket, D.D. Koelling, J. Phys. C: Sol. St. Phys. **13**, 2675 (1980)
34. P. Novak, $WIENROOT/SRC/novak_lecture_on_spinorbit.ps(WIEN97)
35. P. Söderlind, Europhys. Lett. **55**, 525 (2001); P. Söderlind, A. Landa, B. Sadigh, Phys. Rev. B **66**, 205109 (2002)
36. J.G. Gay, J.R. Smith, R. Richter, F.J. Arlinghaus, R.H. Wagoner, J. Vac. Sci. Tech. A **2**, 931 (1984)
37. J.C. Boettger, Phys. Rev. B **49**, 16798 (1994)
38. J.C. Lashley, A.C. Lawson, R J. McQueeney, G.H. Lander, `www.arxiv.org/cond-matt/0410634` (2005)
39. J.C. Boettger, Int. J. Quant. Chem. **95**, 380 (2003)
40. Y. Wang, Y.F. Sun, J. Phys.: Cond. Matt. **12**, L311 (2000)
41. A.B. Shick, V. Drchal, L. Havela, Europhys. Lett. **69**, 588 (2005)
42. T. Durakiewicz, J.J. Joyce, A.J. Arko, D.P. Moore, L.A. Morales, J.L. Sarrao, S. Halas, J. Sikora, W. Krolopp, 61st Annual Physical Electronics Conference (Taos, New Mexico, 2001); T. Durakiewicz, A.J. Arko, J.J. Joyce, D.P. Moore, APS March Meeting 2001, Bull. Am. Phys. Soc. 46, No. 1 (2001)